Proceedings of the 16th International Conference on Soil Mechanics and Geotechnical Engineering

doi:10.3233/978-1-61499-656-9-2193

Loading rate dependency of the subgrade reaction for a pile in liquefied ground

La capacité du taux de charge et la réaction au niveau de la structure en sous-sol d'un pieu planté dans un sol liquéfié

R. Uzuoka
Department of Civil Engineering, Tohoku University, Sendai, Japan

ABSTRACT

The purpose of this study is to clarify the loading rate dependency of subgrade reaction for a single pile in liquefied ground. The parametric studies were performed by incorporating the dynamic soil-pore water coupled formulation and a newly proposed constitutive model. The model can explicitly treat the degree of liquefaction by changing the lower limit of the mean effective stress. The liquefied soil at a certain depth around a pile is modeled with finite elements under the plane stress condition. The subgrade reaction for a pile is calculated under various loading frequencies and degrees of liquefaction. The results of the parametric studies show that the correlation in p-y (subgrade reaction-pile displacement) relations and p-v (subgrade reaction-pile velocity) relations depends on the loading frequency and the degree of liquefaction. The numerical method can reproduce the loading rate dependency of the subgrade reaction for a single pile without the viscosity constitutive model and numerical damping.

RÉSUMÉ

Le but de cette étude est de clarifier la capacité du taux de charge et la réaction au niveau de la fondation en sous-sol d'un simple pieu planté dans un terrain liquéfié. Des études paramétriques sont entreprises grâce à la méthode numérique à laquelle sont associés la dynamique formule des interstices du sol couplée au nouveau modèle constitutif simplifié proposé. Ce modèle-ci peut explicitement traiter le degré de liquéfaction en abaissant la limite de la tension effective moyenne. Le sol liquéfié à une certaine profondeur autour du pieu est modélisé par des éléments finis d'une situation équivalente à celle de la tension crée par un avion. La réaction du pieu au sous-sol est calculée par la prise des données de la charge à différents degrés et fréquences de liquéfaction. Les résultats de cette étude paramétrique montré que la corrélation entre le p-y (un décalage du pieu en sous-sol) et le p-v (la vitesse de réaction du pieu en sous-sol) dépend de la charge en fréquence et en degré de liquéfaction. La méthode numérique peut reproduire la capacité du taux de charge et la réaction en sous-sol d'un simple pieu sans la viscosité du modèle constitutif ou de l'humidification numérique.

1 INTRODUCTION

Liquefaction-induced ground deformation has caused severe damages in pile foundations (e.g. Tokimatsu et al., 1996). The seismic deformation method, which is one of the conventional seismic design methods for piles, uses ground deformation at a particular moment as an external force in order to consider the influence of ground deformation. The design method requires p-y relations, which are the relations between the subgrade reaction and the relative displacement of the ground with respect to the pile. The p-y relations have been investigated with the shaking table tests by many researchers (e.g. Wilson et al., 2000).

In the previous shaking table tests, both p-y and p-v (relative velocity) relations were investigated. The experimental results showed that the subgrade reaction correlated with the relative displacement of the pile with respect to the ground in the case of dense liquefied ground or non-liquefied ground and with the relative velocity of the pile with respect to the ground in the case of loose liquefied ground (Tamura et al., 2000, Suzuki and Adachi, 2002). The loose liquefied ground may behave like a fluid from the viewpoint of correlative p-v relations. Moreover, the strain rate dependency of liquefied sand was examined with laboratory shear tests (Nishimura et al., 2002). However, the behavior of the ground adjacent to the pile has not been clarified since the relative displacement and velocity of the pile were calculated with reference to the displacement and velocity in a free field separated from the pile. In reality, it is difficult to measure the movement of the ground adjacent to a pile through normal shaking table tests.

The purpose of this study is to clarify the loading rate dependency of the subgrade reaction for a single pile in liquefied ground through numerical analyses. The numerical analysis possesses the following features: 1) A simplified non-viscosity constitutive model for liquefied sand, and 2) A dynamic soil-pore water coupled formulation without numerical damping such as Rayleigh damping. The liquefied soil at a certain depth around a pile is carefully modeled with plane stress finite elements. The subgrade reaction for a pile is calculated under various loading frequencies and degrees of liquefaction.

2 NUMERICAL METHOD

The field equations and the proposed constitutive model for liquefied sand are briefly described.

2.1 *Field equations*

In this study, a soil-water coupled problem is formulated based on a u-p formulation (Oka et al., 1994). The finite element method (FEM) is used for the spatial discretization of the equilibrium equation, while the finite difference method (FDM) is used for the spatial discretization of the pore water pressure in the continuity equation. Oka et al. (1994) verified the accuracy of the proposed numerical method through a comparison of numerical results and analytical solutions for transient response of saturated porous solids. The governing equations are formulated by the following assumptions; 1) the infinitesimal strain, 2) the smooth distribution of porosity in the soil, 3) the small relative acceleration of the fluid phase to that of the solid phase compared with the acceleration of the solid phase, 4) incompressible grain particles in the soil.

2.2 *Constitutive model for liquefied sand*

A simplified constitutive model for liquefied sand is proposed. An existing constituting model (Oka et al., 1999) is modified in

order that the model can explicitly treat degree of liquefaction with a changing of the lower limit of mean effective stress. The proposed constitutive model possesses the following features.

2.2.1 *Yield function and hardening rule*

The yield function is expressed as:

$$f = \left\{\left(\eta_{ij}^* - \chi_{ij}^*\right)\left(\eta_{ij}^* - \chi_{ij}^*\right)\right\}^{1/2} - k = 0 \tag{1}$$

$$\eta_{ij}^* = s_{ij} / \sigma_m' \tag{2}$$

where σ_m' is the mean effective stress, s_{ij} is the deviatoric stress tensor, k is the numerical parameter which defines a elastic region and χ_{ij}^* is the kinematic hardening parameter. With nonlinear kinematic hardening rule the increment of χ_{ij}^* is given by

$$d\chi_{ij}^* = B^*\left(M_f^* de_{ij}^P - \chi_{ij}^* d\gamma^{P*}\right) \tag{3}$$

$$d\gamma^P = \left(de_{ij}^P de_{ij}^P\right)^{1/2} \tag{4}$$

where B^* is the material parameter of hardening function, M_f^* is the failure stress ratio and de_{ij}^P is the plastic deviatoric incremental strain tensor.

2.2.2 *Flow rule and plastic potential function*

With non-associated flow rule the plastic potential function is expressed as:

$$g = \left\{\left(\eta_{ij}^* - \chi_{ij}^*\right)\left(\eta_{ij}^* - \chi_{ij}^*\right)\right\}^{1/2} + \tilde{M}^* \ln\left(\sigma_m' / \sigma_{ma}'\right) = 0 \tag{5}$$

where σ_{ma}' is a constant and $\tilde{M}^*$ is defined as follows:

$$\tilde{M}^* = \begin{cases} M_m^* & \eta^* \geq M_m^* \\ \eta^* & \eta^* < M_m^* \end{cases} \tag{6}$$

$$\eta^* = \left(\eta_{ij}^* \eta_{ij}^*\right)^{1/2} \tag{7}$$

where M_m^* is the stress ratio η^* when the maximum compressive volumetric strain occurs during the shearing (phase transformation stress ratio). The liquefied soil is treated at the initial condition in this analysis; therefore plastic volumetric strain due to dilatancy is assumed to be zero when η^* is less than M_m^* as shown in equation (6).

2.2.3 *Parameters for degree of liquefaction*

It is assumed that degree of liquefaction is related to the amount of volumetric strain with dissipation of excess pore water pressure after liquefaction. The volumetric strain after liquefaction depends on the density of sand and the strain history (Sento et al., 2004). The looser sand is, the larger the volumetric strain becomes. The more strain history causes the larger volumetric strain. Assuming that liquefaction process is in overconsolidation region, we can use the following stress-strain relation during the dissipation process of excess pore water pressure:

$$d\sigma_m' = \frac{(1+e_0)\sigma_m'}{\kappa} d\varepsilon_{ii}^e = K d\varepsilon_{ii}^e \tag{8}$$

$$\sigma_m' \geq \sigma_{ml}' = R_{\lim}\sigma_{m0}' \tag{9}$$

where $d\sigma_m'$ is the incremental mean effective stress, σ_{ml}' is the minimum effective stress during liquefaction, e_0 is the initial void ratio, κ is the swelling index, $d\varepsilon_{ii}^e$ is the incremental elastic volumetric strain, K is the bulk modulus, $R_{\lim}$ is the ratio of σ_{ml}' for σ_{m0}' and σ_{m0}' is the initial mean effective stress. Sento et al. (2004) changed σ_{ml}' with the density of sand and strain history, and reproduced the volumetric strain of liquefied sand with equation (8). The small σ_{ml}' means the severe degree of liquefaction. We use equation (8) for the calculation of elastic volumetric strain in the framework of elasto-plastic model. Poisson's ratio is used as another elastic coefficient. The minimum effective stress σ_{ml}' is the lower value of mean effective stress in this analysis, and is also the initial value of mean effective stress. It is noted that the σ_{ml}' has a physical meaning in this study, although the σ_{ml}' has been treated as a numerical parameter in past liquefaction analyses.

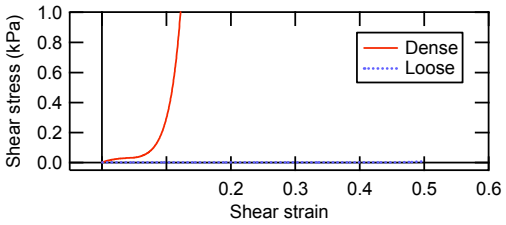

(a) Relations between shear strain and shear stress

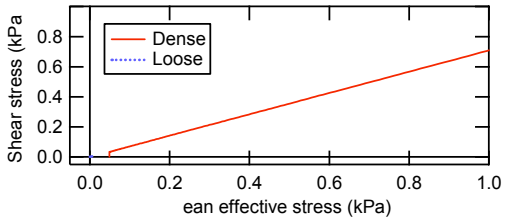

(b) Effective stress paths

Figure 1. Performance of the constitutive model

Table 1. Material parameters

Soil type		Dense sand	Loose sand
Density	ρ (t/m^3)	1.93	1.93
Initial void ratio	e_0	0.60	0.80
Swelling index	κ	0.002	0.003
Poisson's ratio	ν	0.0	0.0
Failure stress ratio	M^*_f	1.00	0.95
Phase transformation stress ratio	M^*_m	0.91	0.91
Hardening parameter	B^*	70	15
itial value of σ'm	σ'_{m0} (kPa)	49	49
arameter for degree of liquefaction	R_{lim}	1.0×10^{-2}	1.0×10^{-8}

2.2.4 *Performance of the constitutive model*

Undrained monotonic torsional shear tests after cyclic shearing were simulated to validate the proposed constitutive model. Figure 1 shows the calculated stress strain behavior for loose Toyoura sand (the relative density of 30 %) and dense Toyoura sand (the relative density of 70 %). Toyoura sand is a fine uniform sand, a mean diameter D_{50} of 0.16 mm and a uniformity coefficient U_c of 1.2. The material parameters for both cases are shown in Table 1. These parameters were determined based on the results of past laboratory tests (Yoshida et al., 1994).

In the case of dense sand, the shear stress and mean effective stress recover due to the dilatancy in the strain region of over about 10 %. In the case of loose sand, the shear stress slightly recovers in the strain region of over 50 %. The effective stress path of loose sand is displayed as a point near the origin. These different behaviors between loose and dense sand are mainly due to the different minimum effective stress. The minimum effective stress of dense sand is 10^5 times larger than that of loose sand. We can easily treat the change in the density and degree of liquefaction with the minimum effective stress in this model.

3 NUMERICAL CONDITIONS OF PARAMETRIC STUDY

Figure 2 shows the concept of analytical model and the finite element model. The horizontal plane around a single pile at a certain depth is treated. The dimensions of the finite element model are 10 m × 10 m × 0.05 m, and the diameter of the pile is 0.5 m. The soil around the pile is modeled with isoparametric elements, and the pile is assumed to be rigid. The lateral boundaries are fixed in the horizontal directions, and the bottom boundary is fixed in all directions. The effective overburden pressure before liquefaction is 49 kPa, and the vertical total stress keeps constant. All boundaries are impermeable and the seepage between neighboring elements is not treated.

All solid elements are modeled with proposed constitutive model for liquefied sand. In the initial state, all elements completely liquefy. The effective stress is isotropic, and is assumed to be the minimum effective stress. Moreover, the excess pore water pressure ($\sigma'_{m0} - \sigma'_{ml}$) is generated. We consider two cases for the degree of liquefaction, light degree ($R_{\lim} = 10^{-2}$) and medium degree ($R_{\lim} = 10^{-5}$), as shown in Table 2.

A sinusoidal wave of input acceleration is set at the nodes on the edge of the pile. Three cases of frequencies of 0.1 Hz, 1.0 Hz and 10.0 Hz are treated. The amplitude of displacement is 2.5 mm (0.5 % of the diameter of the pile), which corresponds the amplitude generated in the shaking table tests (Tamura et al., 2000). The dilatancy of this model is not very significant in this range of displacement. The incremental displacement of the calculation is 1/125 of 2.5 mm for all cases.

4 NUMERICAL RESULTS OF PARAMETRIC STUDY

The relations between the calculated subgrade reaction and the pile displacement (p-y relations), and the relations between the calculated subgrade reaction and the pile velocity (p-v relations) are discussed with respect to the degrees of liquefaction and loading frequencies. The subgrade reaction is the sum of the nodal forces at the nodes on the edge of pile. The value of subgrade reaction is converted to that for the depth of 1.0 m.

4.1 *Influence of loading frequency on p-y and p-v relations*

The p-y and p-v relations and the time histories of subgrade reaction and inertia force for the cases of c-h1, c-h2 and c-h3 are shown in Figure 3, 4 and 5 respectively. The displacement and velocity of the pile are the relative amplitudes to the fixed edge of the finite element model; therefore they correspond to the relative amplitudes with respect to the free field responses. The inertia force is the product of the additional mass around the pile and the input acceleration. The additional mass is the sum of the lumped mass at the nodes of pile distributed from the neighboring soil elements.

In the slowest case of c-h1 (Figure 3), the p-y relation has a positive correlation, and the p-v relation has no clear correlation. The inertia force is much smaller than the subgrade reaction. In the medium fast case of c-h2 (Figure 4), on the other hand, the p-y relation has no clear correlation, and the p-v relation has positive correlation. The amplitude of inertia force is about a half of that of subgrade reaction, and the phase of subgrade reaction is slower than that of c-h1. In the fastest case of c-h3 (Figure 5), the p-y relation has negative correlation, and the p-v relation has positive correlation with large hysteresis. The inertia force is much larger than the subgrade reaction, which coincides with negative correlation in the p-y relation. Moreover, the wave shape of subgrade reaction is different from the other cases. These results clearly show that the correlation in the p-y and p-v relation changes with the loading rate.

The p-y and p-v relations in the case of c-h1 and c-h2 are almost linear because the generated strain in the surrounding ground is not large. The similar results are obtained when the amplitude of displacement is 50.0 mm (10 % of the diameter of

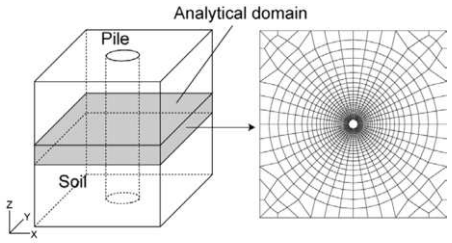

Figure 2. Concept of the numerical model

Table 2. Numerical cases

Degree of liqeufaction	Loading frequency		
	0.1Hz	1.0Hz	10.0Hz
Light: $R_{lim}=10^{-2}$	c-h1	c-h2	c-h3
Medium: $R_{lim}=10^{-5}$	c-m1	c-m2	c-m3

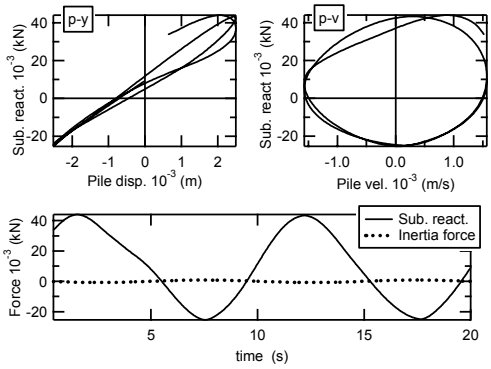

Figure 3. P-y and p-v relations and time histories of subgrade reaction and inertia force (case c-h1)

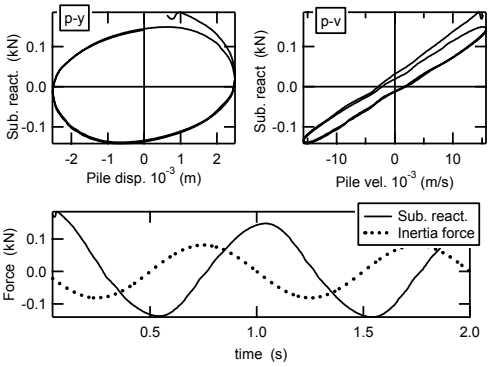

Figure 4. P-y and p-v relations and time histories of subgrade reaction and inertia force (case c-h2)

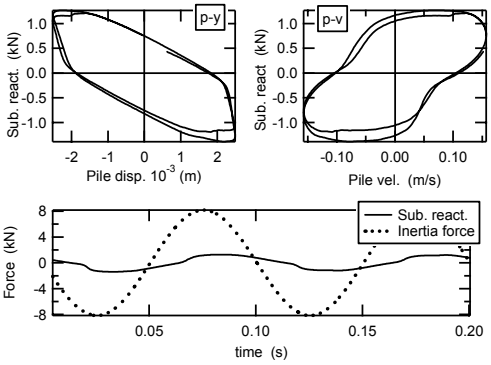

Figure 5. P-y and p-v relations and time histories of subgrade reaction and inertia force (case c-h3)

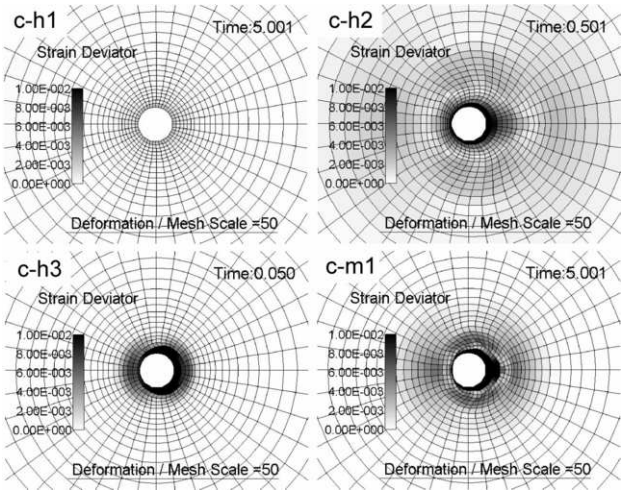

Figure 6. Deformed configuration and distribution of strain deviator (case c-h1, c-h2, c-h3 and c-m1)

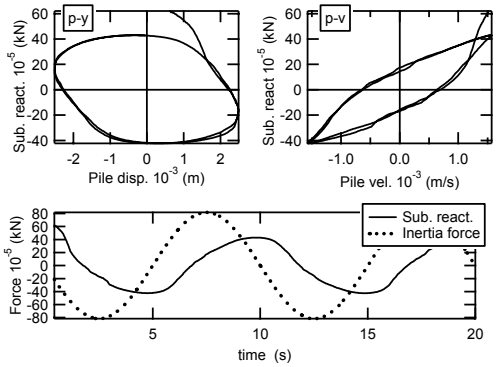

Figure 7. P-y and p-v relations and time histories of subgrade reaction and inertia force (case c-m1)

the pile) although the p-y and p-v relations show hysteresis and slight hardening.

Figure 6 shows the deformed configuration and the distribution of strain deviator for the cases of c-h1, h2 and h3. The strain deviator is the cumulative value with equation (4). These figures are output at the time (T1) when a half period of input sinusoidal wave passed and the pile displacement is zero. The deformation scale is 50 times larger than the mesh scale. In the case of c-h1, the surrounding ground around the pile returns to the original position as well as the pile. This result means that the surrounding ground moves with the same phase as the pile, which causes positive correlation in the p-y relation. In the case of c-h2, the surrounding ground remains deformed although the pile returns to the original position. There is a phase difference between the movements of the surrounding ground and the pile. Moreover, the area with large strain deviator is larger than that of other cases. The loading frequency of 1.0 Hz is possible to be close to the natural frequency of the surrounding ground. This phase difference causes positive correlation in the p-v relation as shown in Figure 4. In the case of c-h3, only the ground adjacent to the pile remains deformed. The area with large strain deviator is localized near the pile because this area is affected by the large inertia force from the neighboring ground.

4.2 *Influence of degree of liquefaction on p-y and p-v relation*

Figure 7 shows the p-y and p-v relations and the time histories of subgrade reaction and inertia force for the case of c-m1. As the degree of liquefaction becomes more severe, the p-v relation has a positive correlation with the lower loading frequency. The stiffness of liquefied ground in this case is smaller than that of the case of c-h1. Hence, the natural frequency becomes small, and this case shows the similar behavior as the case of c-h1. The deformed configuration in this case is also similar to that in the case of c-h1 as shown in Figure 6. These results clearly show that the correlation in the p-y and p-v relation changes with the degree of liquefaction.

5 CONCLUSIONS

The loading rate dependency of the subgrade reaction of a pile in liquefied ground is discussed through numerical analyses. A simplified non-viscous constitutive model for sand is incorporated with the soil-water coupled formulation. The numerical results reveal the following:

1) The correlation in the p-y and p-v relations depends on the loading frequency and degree of liquefaction. The surrounding ground moves with a phase that is different from that of pile movement under a particular condition, which causes positive correlation in the p-v relation.
2) The loading rate dependency of the subgrade reaction of a pile in liquefied ground can be reproduced by the dynamic analysis without the viscous constitutive model and numerical damping.

In this study, the horizontal plane was the only object under consideration; however, the response of liquefied ground and pile also changes along the vertical direction. We require further investigations into the 3-dimensional behavior of the pile and the ground.

ACKNOWLEDGEMENT

This study was supported by the research grant of Japan Iron and Steel Federation in FY2002-2003. Miss Minako Shibasaki, formerly graduate student of Tohoku University, carried out the numerical analyses. The author wishes to thank them for their cooperation.

REFERENCES

Nishimura, S., Towhata, I. and Honda, T. 2002. Laboratory shear tests on viscous nature of liquefied sand, *Soils and Foundations*, 42, 4, 89-98.

Oka, F., Yashima, A., Shibata, T., Kato, M. and Uzuoka, R. 1994. FEM-FDM coupled liquefaction analysis of a porous soil using an elasto-plastic model, *Applied Scientific Research*, 52, 209-245.

Oka, F., Yashima, A., Tateishi, A., Taguchi, Y. and Yamashita, S. 1999. A cyclic elasto-plastic constitutive model for sand considering a plastic strain dependency of the shear modulus, *Geotechnique*, 49, 5, 661-680.

Sento, N., Kazama, M. and Uzuoka, R. 2004. Experiment and idealization of the volumetric compression characteristics of clean sand after undrained cyclic shear, *J. Geotechnical Engineering, JSCE*, 764/III-67, 307-317. (in Japanese)

Suzuki, Y. and Adachi, N. 2003. Relation between subgrade reaction of pile and liquefied ground response, *Proc. 38th Japan National Conf. on Geotechnical Engineering*, Akita, 1945-1946. (in Japanese)

Tamura, S., Kobayashi, K., Suzuki, Y. and Yoshizawa, M. 2001. Relation between pile behavior and subgrade reaction based on pile vibration test using large-scale laminar box, *Proc. 36th Japan National Conf. on Geotechnical Engineering*, Tokushima, 1711-1712. (in Japanese)

Tokimatsu, K., Mizuno, H and Kakurai, M. 1996. Building damage associated with geotechnical problems, *Soils and Foundations*, *Special Issue on Geotechnical Aspects of the January 17 1995 Hyogoken-Nambu Earthquake*, No.1, 219-234.

Wilson, D. W., Boulanger, R. W. and Kutter, B. L. 2000. Observed seismic lateral resistance of liquefying sand, *Journal of Geotechnical and Geoenvironmental Engineering, ASCE*, 126, 10, 898-906.

Yoshida, N., Yasuda, S., Kiku, M., Masuda, T. and Finn, W.D.L. 1994. Behavior of sand after liquefaction, *Proc. from the 5th U.S.-Japan Workshop on Earthquake Resistant Design of Lifeline Facilities and Countermeasures Against Soil Liquefaction*, Utah, 181-198.